Final Performance Report

Multi-Ferroic Polymer Nanoparticle Composites for Next Generation Metamaterials

Grant FA2386-14-1-4086

Peter Kofinas

Fischell Department of Bioengineering, University of Maryland, College Park, MD 20742, USA

Abstract

Stretchable magneto-dielectric composites were prepared using collectively assembled iron oxide nanoclusters as fillers in an elastomer (polydimethylsiloxane) matrix. Raspberry-shaped nanoclusters (RSN) of iron oxides with different structures and compositions were synthesized by oriented aggregation of nanocrystals. This collectively assembled structure improved crystal quality and prevented the formation of surface and volume spin canting, leading to low coercivity iron oxide nanomaterials with enhanced saturation magnetization (M_S). The improved magnetization and low coercivity of the filler material allowed the fabrication of magneto-dielectric composites that can combine permeability values reaching 2.3 with magnetic loss values limited to 0.11. The resulting composites can also be stretched up to 165% strain before failure due to good adhesion between the elastomer and citrate capped RSNs. In addition, the composition of these fillers was altered to adjust the resonance frequency of the resulting composite material. Stretchable magneto-dielectric composites consisting of maghemite-rich RSNs and magnetite-rich RSNs demonstrated resonance frequencies similar to the spherical ferromagnetic resonance of maghemite and magnetite, respectively.

Introduction

Nanostructured polymer-nanoparticle composites have been widely used as conductive and dielectric materials for applications in flexible electronics.[1] In particular dielectric polymer-nanoparticle composites with high dielectric constant (ε) and permeability (μ) with low dielectric and magnetic loss show promise in the future development of flexible and compact radio frequency (RF) devices.[1e, 2] These composites referred to as flexible magneto-dielectrics utilize magnetic nanoparticle fillers to achieve high permeability and permittivity, while the polymer matrix provides mechanical elasticity, robustness, and separation between nanoparticles to prevent formation of conductive losses.[1e, 2-3]

The magnetic properties of the dispersed nanoparticles have significant influence on the frequency dependent electromagnetic properties of magneto-dielectric composites.[4] The permeability of a magneto-dielectric composite is directly proportional to the saturation magnetization of the nanoparticles.[4] Additionally, incorporating nanoparticles with higher magnetic anisotropy in composites results in materials with increased magnetic loss.[4-5] Another important consideration is the magnetic resonance frequency of the composites, which is determined by the magnetic resonance frequency of the nanoparticles.[5] The permeability of the composite reaches a maximum at its resonance frequency, and decreases significantly for frequencies beyond the magnetic resonance, which is governed by the Snoek's limit.[6] The optimal magneto-dielectric composite for high efficiency RF devices thus contains magnetic nanoparticles with high saturation magnetization, low coercivity, and tunable magnetic resonance frequency.

Iron oxide materials such as magnetite and maghemite show promise as magnetic fillers for large scale magneto-dielectric polymer-nanoparticle composite production, because of their low manufacturing cost, high bulk saturation magnetization (M_s), and size dependent coercivity.[7] Additionally, it is possible to adjust the magnetic resonance of the iron oxides by tuning the structure and composition.[5, 8] However, iron oxide fillers prepared as nanoparticles to minimize coercivity exhibit magnetization values significantly lower than their bulk M_s, as a result of stoichiometric impurities and defects.[9] Thus, it is extremely difficult to obtain composites with high μ values, and low magnetic loss using iron oxide nanoparticles.[2a, 2c, 8] It has been recently reported that it is possible to enhance the limited magnetic properties of magnetite nanoparticles by synthesizing nanostructures consisting of oriented aggregates of iron oxide nanocrystals.[10] These nanostructures are composed of nanocrystals with common crystallographic orientations combined together to form nanoclusters. Such nanostructures are generally synthesized using polyol methods, which have been demonstrated as an easy and consistent way to synthesize "raspberry"-shaped nanostructures (RSN).[10c-e, 11] Nanocrystal clusters with sizes ranging from tenth of nanometers to 800 nm and crystal size between 5 to 20 nm have been synthesized by tuning reaction condition parameters such as solvents,[10b, 12] reaction time,[11a] pH[13] or stabilizing agent.[13-14] This size adjustable raspberry-like nanostructure leads to collective magnetization

effects, which allows these nanostructures to match the M_s of bulk magnetite without significantly increasing the magnetic anisotropy of the material.[10b-e]

In this work, we demonstrate a stretchable magneto-dielectric composite with high permeability, low magnetic and dielectric loss, and adjustable magnetic resonance frequency by using iron oxide RSNs as the filler material. Iron oxide RSNs form collectively assembled magnetic nanoclusters with high M_s and low coercivity, which improves the permeability of the composites without significantly increasing their magnetic loss. In addition to beneficial magnetic characteristics, iron oxide RSNs can be assembled from nanoparticles with different phases of magnetic iron oxide, which have distinct natural magnetic resonance. This hybrid structure enables fabrication of composites with different magnetic resonance frequency, which is determined by the nature of the major iron oxide composition of the RSN filler.

The iron oxide RSNs have been synthesized by one-pot solvothermal synthesis following a modified polyol solvothermal method. The reaction time is used to alter the structure, composition and magnetic properties of the filler iron oxide RSNs. The solvothermal syntheses with reaction periods of 7 and 13 hours, result in spherical hollow clusters of iron oxide nanocrystals with a mean crystal size of 5 and 25 nm, respectively. The smaller crystal size particles consist mostly of maghemite (γ-Fe_2O_3), while the larger crystal size particles have a magnetite (Fe_3O_4) rich composition. Both types of RSNs have been chemically functionalized with a citrate-capping agent to favor their dispersion in polydimethylsiloxane (PDMS) matrix. The citrate capped RSNs with different composition and structure were dispersed in PDMS matrix, which was subsequently cross-linked to form magnetite- and maghemite-rich magneto-dielectric composites. The magnetite- and maghemite-rich magneto-dielectric composites could be stretched up to 165%. Additionally, both composites have demonstrated permeability values exceeding 2 with loss values remaining below 0.1 below the magnetic resonance frequency. The maghemite-rich magneto-dielectric composites have a magnetic resonance centered at 500 MHz. On the other hand, magnetite-rich composites have demonstrated a magnetic resonance slightly higher than 1 GHz. The difference in magnetic resonance frequency of the composites is potentially originating from the different composition of the filler materials, as the experimental magnetic resonance frequency of the composites were found to be close to the theoretical natural magnetic resonance of the dominant iron oxide phase in their filler material.

I. Experimental section

Materials

Hexahydrate iron (III) chloride ($FeCl_3$, $6H_2O$), urea and ethylene glycol were purchased from Alfa Aesar with purity of 97%, 99.3% and 99%, respectively. Succinic acid (SA) was purchased from Sigma-Aldrich with a purity of ≥99.5%. Sylgard 184 of Dow Corning was used as the uncured polydimethylsiloxane (PDMS) matrix.

Synthesis of raspberry nanostructures (RSN)

In a typical synthesis $FeCl_3$, $6H_2O$ (30 mmol), succinic acid (10 mmol) and urea (300 mmol) were completely dissolved in ethylene glycol (300 ml) by vigorous mechanical stirring and sonication. The solution was sealed in a Teflon lined stainless steel autoclave, slowly heated at 200°C at 1.5°C/min and kept at this temperature for 7 or 13 hours. The autoclave was cooled down to room temperature afterwards by water circulation during 1 h. The powders were separated by centrifugation and washed 3 times with ethanol and 3 times with deionized water to eliminate organic and inorganic impurities. Finally, the powders were freeze-dried to remove water and a black powder was obtained (1500 mg).

Citrate functionalization of raspberry nanostructures (RSN)

RSNs were coated with citrate molecules using a similar procedure previously reported.[15] A 250 ml buffer solution (pH 5) of citric acid (0.14 $mol.l^{-1}$) and potassium citrate (0.26 $mol.l^{-1}$) was prepared. Then, RSNs (1.5 g) were immersed in the solution and stirred for 1 hour to promote the nanoparticle surface coating. After stirring, the RSNs were extracted and washed once by centrifugation with deionized water to remove any excess of citric acid. Finally, the powders were freeze-dried to remove water.

Fabrication of magneto-dielectric composites

PDMS (Sylgard 184, Dow Corning) was prepared by mixing base silicone polymer with a curing agent in a 10:1 weight ratio. Dry RSNs were mixed in the polymer at the desired nanoparticle loading. The polymer particle mixture was poured into a mold, placed in a vacuum desiccator for 30 minutes to remove air bubbles, and cured at 100 °C for 4 hours.

Characterization

Sizes, morphologies and crystal structures were characterized by scanning electron microscopy (SEM) with a JEOL 6700F (point resolution 2 nm), a transmission electron microscopy (TEM) with a JEOL ARM200F microscope operating at 200 kV (point resolution 0.18 nm) and a JEOL 2100F electron microscope working with a 200 kV accelerating voltage equipped with a GATAN GIF 200 electron imaging filter. Selected area electron diffraction (SAED) was performed using a JEOL ARM200F microscope.

Dried powders were placed in a platinum crucible. Specific surface areas of the different samples were determined by N_2 adsorption-desorption measurements at 77 K by using a Micromeritics TriStar 3000 apparatus. Before the measurements, samples were outgassed at 150 °C overnight in order to desorb impurities or moisture from their surface.

Global magnetic measurements were recorded with a Superconducting Quantum Interface Device (SQUID) magnetometer (Quantum Design MPMS-XL 5) and Vibrating Scanning Magnetometer (VSM; Lakeshore 7400 series).

The magneto-dielectric properties of the composites were determined using an Agilent RF impedance/material analyzer (E4991A).

II. Results and discussions

The citrate capped RSN filler materials with different structure and composition have been synthesized following a modified polyol solvothermal approach, described in the experimental section. The structure and composition of these filler materials were altered by modulating the reaction time. The structure of the collectively assembled RSN fillers prepared using different reaction duration was characterized with electron microscopy and selected area diffraction (SAED). The scanning electron microscopy (SEM) images revealed that both RSN fillers have an average diameter of 300 nm (Figure 1a, b). The surface roughness apparent in SEM images is indicative of a cluster-like structure. The transmission electron microscopy (TEM) characterization has demonstrated that these nanoclusters possess a hollow core, which confirms the raspberry-like shape of this filler material (Figure 1c, d). We have utilized high-resolution TEM imaging at the interface between two crystals in these RSN filler materials to confirm the collective assembly of the nanocrystals (Figure 1c, d-inset). The TEM images clearly demonstrate that crystallographic orientations of both crystals are matched at the interface, which is indicative of a common crystal orientation shared by nanocrystals forming the RSN fillers. Additionally, the von Laue patterns apparent on SAED measurements supports the existence of a crystal structure with similar crystal orientation for RSN fillers.[10b, 10c] The common crystal orientation, possibly originating from the well known oriented aggregation upon crystal growth,[10b, 10c] and provides strong evidence for the collective assembly of nanocrystals in RSN fillers.[10b-d] The detailed characterization of the microstructure of these collectively assembled nanoclusters of iron oxide fillers has showed that RSN fillers allowed to react for 7 hours have finer crystal size than fillers allowed to react for 13 hours (Figure 1e, f). The powder diffraction studies indicate an average crystal size of 5 nm for RSN fillers reacted for 7 hours and 25 nm for RSN fillers reacted for 13 hours (Figure 2a). The compositions of the respective RSN fillers were investigated using Mössbauer spectroscopy (Figure 2b). This investigation showed that RSN fillers consist of maghemite and magnetite. Mössbauer spectroscopy has shown that RSN fillers with smaller crystal size have demonstrated a maghemite-rich composition ($Fe_{2.78}O_4$, 70% of maghemite). RSN fillers with large crystal size are mainly constituted of magnetite Fe_3O_4 phase ($Fe_{2.90}O_4$, 70% of magnetite). These variations in composition can be explained by the surface oxidation of magnetite, which might be elevated due to smaller crystal size of maghemite-rich RSN fillers.[12]

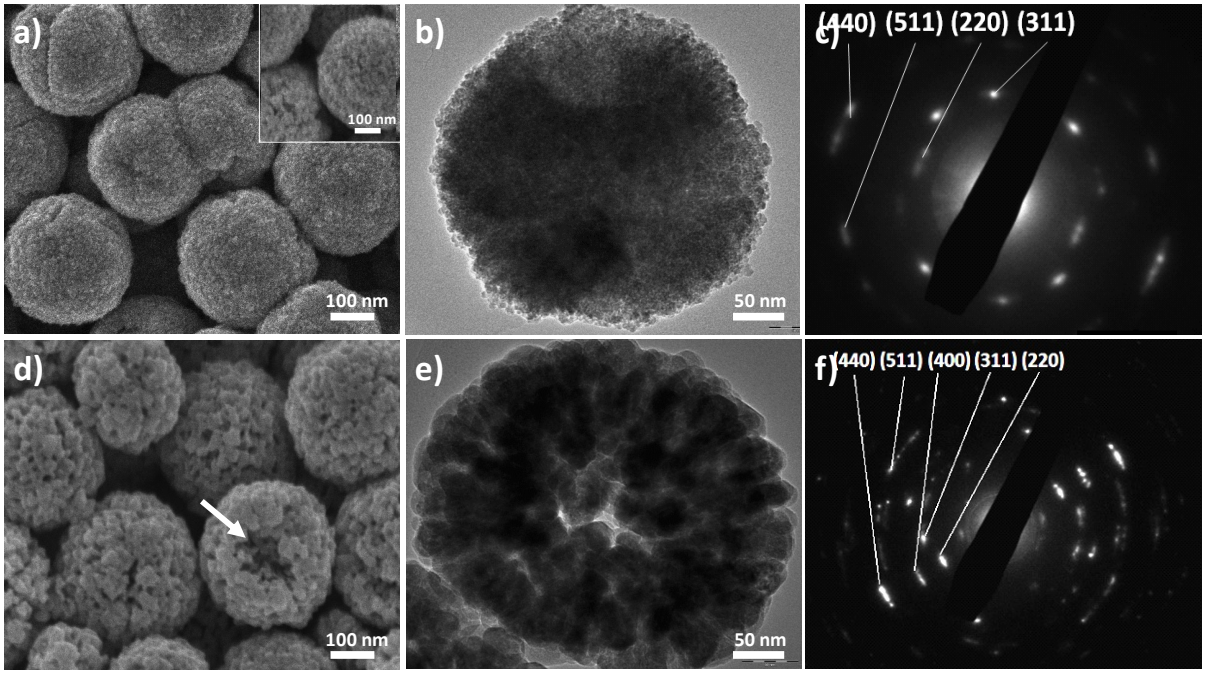

Figure 1. Citrated iron oxide with raspberry-shaped nanostructure. a), b), c) RSN5. d), e), f) RSN25. a), d) SEM micrographs. b), e) TEM micrograph. c), f) Electron diffraction pattern.

The characterization of the magnetic properties of RSN fillers correlates well with their structure and composition. The magnetite-rich RSNs have demonstrated a M_s of 88 emu/g, which is comparable to the bulk M_s of magnetite (92 emu/g) (Figure 3a).[10b] In contrast to magnetite-rich RSNs, stoichiometric magnetite nanoparticles have a saturation magnetization between 45 emu/g and 55 emu/g due to poor crystalline order, and deteriorating influence of surface and volume spin canting.[5, 7a, 9a, 9b] In fact, the structure of RSNs, which display aggregated orientation of nanocrystals have a critical role for improving the structural and magnetic order, limiting the influence of surface and volume spin canting.[9b, 9c, 10a, 10b, 11b] The strong dipolar interactions between nanocrystals forming RSNs favors the coupling of spins at the grain surface, which reduces the magnetic and structural disorder arising commonly from defects or broken bonds in the surface of iron oxide nanocrystals.[9b, 10a] The spin coupling at the interface helps minimizing the influence of spin canting for RSNs consisting of nanocrystals with an average size smaller than 5 nm, in which the surface spin canting dominates over volume effects.[9b, 10a] In addition, the coalescence of crystals during the synthesis of RSNs results in grains with same crystallographic orientation, which induces collective magnetic properties for RSNs.[10a, 10b] The common crystallographic orientation is also beneficial to limit the volume spin canting, as it promotes a single structural and magnetic order with minimum amount of defects.[9b, 9c] Because of the strong dipolar interactions between nanocrystals, and the common crystallographic orientation of grains, RSNs exhibit higher crystal quality, and lower spin canting than iron oxide nanoparticles, which leads to magnetization values matching bulk materials. Similarly, the maghemite-rich RSNs exhibit a M_s (74 emu/g) comparable to the M_s of bulk maghemite (81 emu/g) (Figure 3b).[9b] This

high magnetization is possibly originating from the collective assembly of nanocrystals instead of an increase in crystal size, since the coercivity of both magnetite- and maghemite-rich RSNs remains below 30 Oe, which is indicative of small crystal size (Figure 3a, b).[9a, 9b]

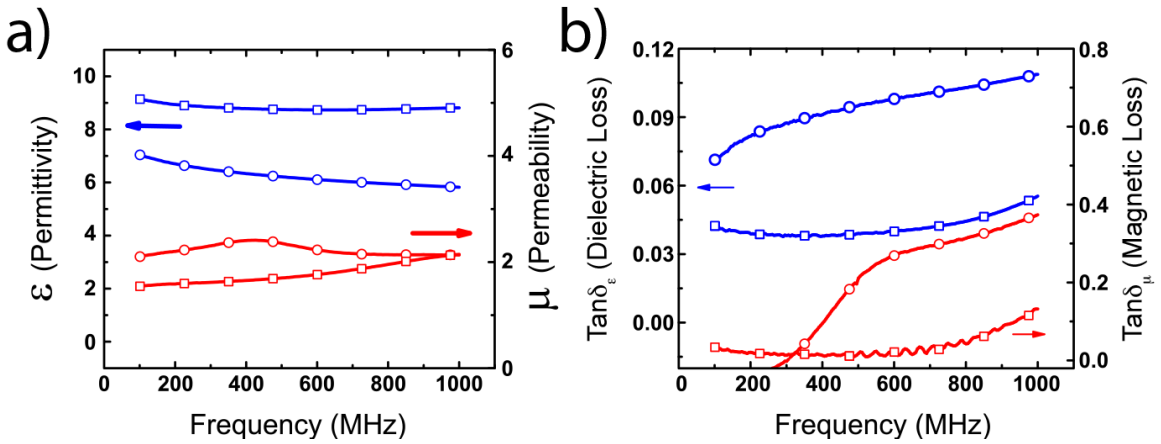

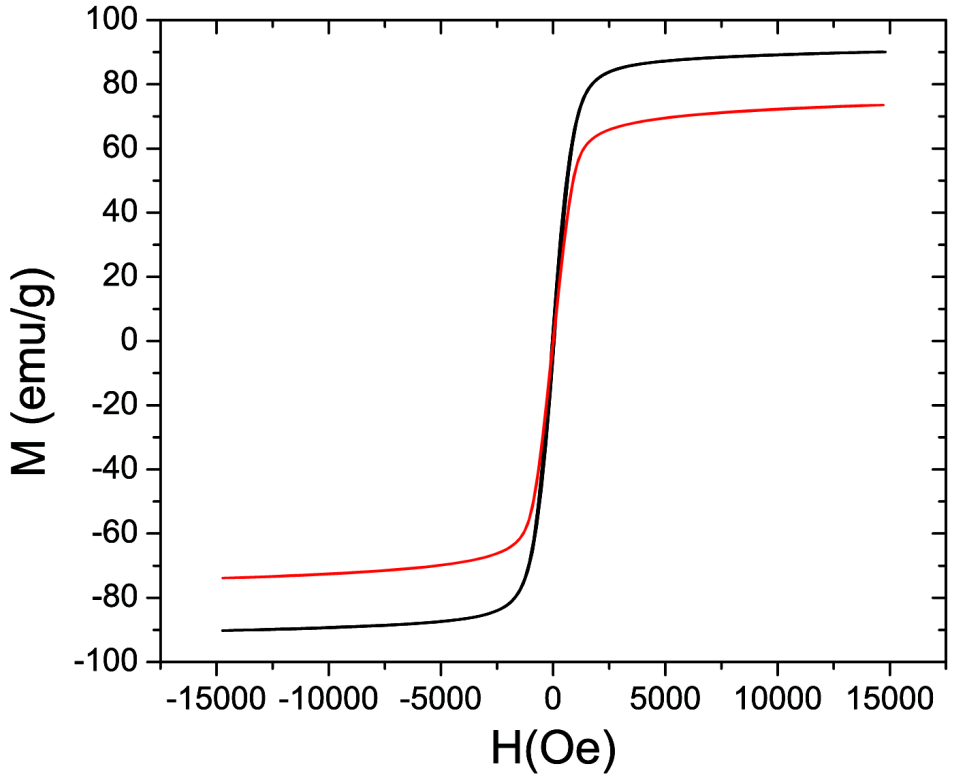

Figure 3. Room temperature magnetization curves for maghemite-rich (red) and magnetite-rich (black) RSNs.

Citrate-capped RSNs with a negative surface charge were easily dispersed in a polydimethylsiloxane (PDMS) elastomer matrix and cross-linked to form stretchable magneto-dielectric composites. Dynamic mechanical analysis was performed to evaluate the mechanical properties of these composites. The elastic modulus, as calculated from stress/strain curves, of stretchable composites prepared with small-grain (1.15 MPa) and large-grain (0.7 MPa) iron oxide nanostructures was higher than that of bare PDMS (0.56 MPa) (Figure 4).[16] This is indicative of favorable interactions between the nanostructures and the PDMS matrix. The elastic modulus was also dependent on grain size. The higher surface area of the small-grain size nanostructures (57.3 m^2/g), in comparison to the large-grain nanostructures (27.3 m^2/g), causes more interactions between filler and matrix material and lead to a higher modulus.[17] Additionally, stretchable composites prepared with small-grain (175%) and large-grain (165%) iron oxide nanostructures demonstrated elongation at break values comparable to bare PDMS (Figure 4).[18]

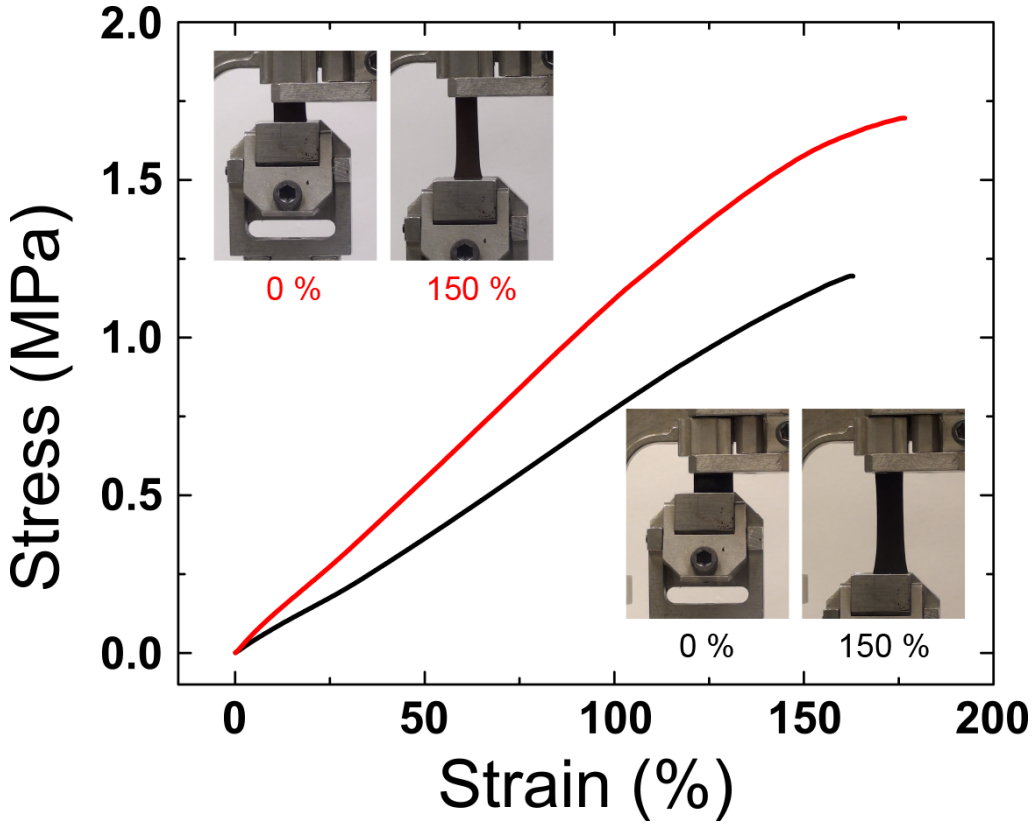

Figure 4. Stress/strain curves for small-grain (red) and large-grain (black) hollow iron oxide nanostructure polymer composites with 60 wt% nanoparticle loading. The images of elongated composites are shown as an inset.

The permittivity (ε), permeability (μ) and electromagnetic loss values for the composites were measured at a frequency range of 1 KHz to 1 GHz. The permittivity values remained stable and free of dielectric resonance and relaxation for both composites in this frequency range (Figure

5a). The composites prepared with large-grain and magnetite-rich RSNs demonstrated permittivity values reaching 9, which is higher than composites prepared with small-grain and maghemite-rich RSNs. Magnetite fillers are known to generate composites with higher permittivity compared to composites prepared with maghemite fillers.[2a, 3b]

Permeability measurements showed a distinct peak with a maximum value of 2.32 centered at 420 MHz for composites with small-grain nanostructures (Figure 5a). The permeability of composites prepared using large-grain iron oxide nanostructures increased with frequency, reaching a maximum permeability value of 2.1 at 1 GHz. The described stretchable magneto-dielectric composites have demonstrated permeability values exceeding that of any reported polymer nanoparticle composites prepared with maghemite[3b] or magnetite[5] nanoparticles using similar filler concentration in this frequency range. We believe the high permeability values achieved by these composites originate from the high saturation magnetization of the hollow iron oxide nanostructures.

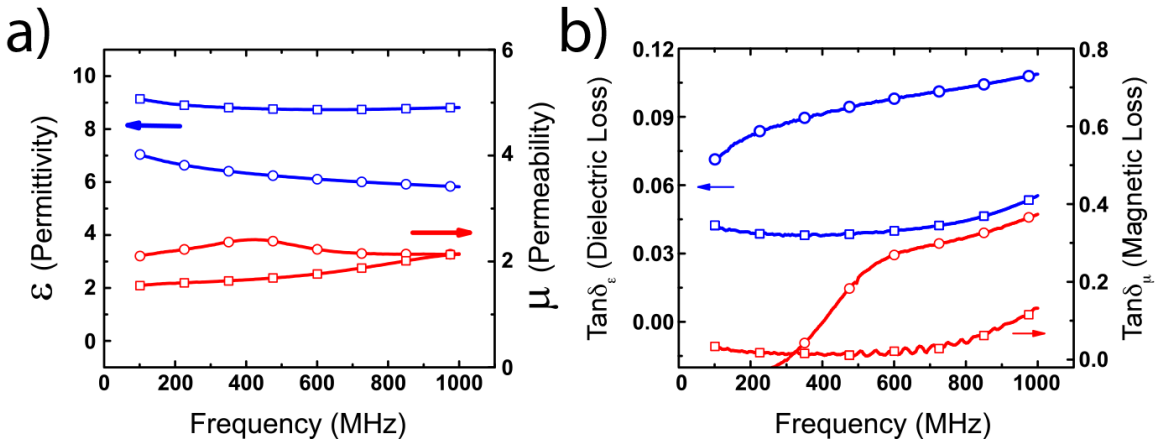

Figure 5. Frequency dependence of (a) permittivity (ε), permeability (μ) and (b) dielectric and magnetic loss values of large grain (squares) and small-grain (circles) hollow iron oxide nanostructure polymer composites with 60 wt% nanoparticle loading.

The dielectric ($\tan\delta_\varepsilon=\varepsilon'/\varepsilon''$) and magnetic ($\tan\delta_\mu=\mu'/\mu''$) loss values for composites were measured to investigate electromagnetic loss characteristics and resonances at the frequency range of interest (1 KHz to 1 GHz). The dielectric loss values of composites fabricated using both maghemite-rich small-grain and magnetite-rich large-grain RSNs do not demonstrate a dielectric resonance in the range 1 KHz to 1 GHz. Additionally, dielectric loss values remain below 0.1 for either composite. The frequency dependence of magnetic loss values for composites prepared with maghemite-rich small-grain RSNs show local maxima between 400 MHz and 600 MHz, as the slope of the curve drops drastically at 500 MHz, which is indicative of a magnetic resonance (Figure 5b). This local maxima is masked by the presence of a second magnetic resonance at frequencies higher than 600 MHz, which could potentially be caused by the structure oriented gyromagnetic resonance reported at 1.5 GHz for maghemite nanoparticles.[19] The magnetic loss characterization of composites prepared with the magnetite-rich RSNs show an increase in loss values between 600 MHz and 1 GHz. In concert with permeability measurements, the magnetic

loss measurements indicate a magnetic resonance at a frequency slightly higher than 1 GHz. Further characterization revealed that the magnetic loss value for composites assembled with maghemite-rich RSNs was 0.11 at 420 MHz. Composites prepared with magnetite-rich RSNs had a magnetic loss value of 0.13 at 1 GHz.

The theoretical ferromagnetic resonance frequency of spherical maghemite and magnetite is calculated to identify the origin of the magnetic resonances in these magneto-dielectric composites.[20]

$$f_r = \gamma H_k$$

The magnetocrystalline anisotropy field (H_k) is calculated by assuming cubic symmetry for both maghemite and magnetite particles.[5, 21]

$$H_k = \frac{2|K_1|}{\mu_0 M_S}$$

The gyromagnetic ratio ($\gamma/2\pi$) of electrons was used for these calculations (28 GHz/T).[20] Magnetocrystalline anisotropy constant (K_1), saturation magnetization (M_S) values along with calculated ferromagnetic resonance frequencies for maghemite and magnetite nanoparticles are given in Table 1.

Table 1:

	Maghemite nanoparticles [21]	Magnetite nanoparticles [5]
K_1 (J/m^3)	$4.6x10^3$	$-1.2x10^4$
M_S (A/m)	$4x10^5$	$4.6x10^5$
Theoretical f_r (MHz)	480 MHz	1.46 GHz
Experimental f_r (MHz)	600 MHz	1.3 GHz

Previous experimental studies have demonstrated that ferromagnetic resonance frequency for maghemite nanoparticles is 600 MHz, which is slightly higher than the theoretical ferromagnetic resonance of maghemite nanoparticles, and maghemite-rich magneto-dielectric composites.[21] In addition, the experimentally determined ferromagnetic resonance frequency for magnetite nanoparticles is 1.3 GHz, which is slightly lower than theoretical ferromagnetic resonance frequency of magnetite nanoparticles.[5] The difference in calculated resonance frequencies of magnetite and maghemite nanoparticles, and experimentally determined resonance conditions for the type of nanoparticle, and RSN based composites possibly originate from the heterogeneous composition of filler materials, which leads to changes in the magnetocrystalline anisotropy constants.[5, 21-22]

The permeability peak at 420 MHz, and the drastic increase in magnetic loss from 400 MHz to 600 MHz for composites prepared with maghemite-rich RSNs (small grains) are most probably stemming from the ferromagnetic resonance of maghemite at 480 MHz. In addition, the increase in permeability and magnetic loss starting from 600 MHz for composites consisting of magnetite-rich RSNs (large grains) can be explained by the natural ferromagnetic resonance of magnetite (1.46 GHz) as the permeability and magnetic loss starts to increase prior to resonance frequency. [5] Therefore, it is possible that the composition of the filler material defines the magnetic resonance frequency for the composites with large- and small-grain RSNs. This composition dependence can be used to change the magnetic resonance frequency of the composites by altering the level of oxidation of RSNs with reaction time of the solvothermal synthesis. These low loss values possibly stem from limited coercivity of the iron oxide nanostructures.

III. Conclusion

In summary, stretchable magneto-dielectric composites with high permeability, low magnetic loss were demonstrated using iron oxide RSN fillers with high M_s and low coercivity. Iron oxide RSN fillers consisting of magnetic nanocrystals aggregated with common crystallographic orientations displaying higher M_s in comparison to individual iron oxide nanoparticles with coercivity values smaller than 30 Oe. This allowed magneto-dielectric composites to achieve permeability values reaching 2.3 with magnetic loss values that did not exceed 0.4. Iron oxide RSNs with different composition and crystal size have resulted in magneto-dielectric composites with distinct magnetic resonance. Additionally, the citrate capping of iron oxide nanostructures ensured uniform distribution of the filler in the elastomer (PDMS) matrix, which prevented formation of conductive losses in composites and provided the ability to stretch up to 165% strain. Imparted with excellent stretchability these unique magneto-dielectric characteristics provide evidence that such composites can be utilized to fabricate high efficiency flexible antennas operating at distinct RF frequencies.

References

1. (a) Park, M.; Im, J.; Shin, M.; Min, Y.; Park, J.; Cho, H.; Park, S.; Shim, M. B.; Jeon, S.; Chung, D. Y.; Bae, J.; Park, J.; Jeong, U.; Kim, K., Highly stretchable electric circuits from a composite material of silver nanoparticles and elastomeric fibres. *Nat Nanotechnol* 2012, *7* (12), 803-809; (b) Kim, Y.; Zhu, J.; Yeom, B.; Di Prima, M.; Su, X. L.; Kim, J. G.; Yoo, S. J.; Uher, C.; Kotov, N. A., Stretchable nanoparticle conductors with self-organized conductive pathways. *Abstr Pap Am Chem S* 2014, *248*; (c) Balazs, A. C.; Emrick, T.; Russell, T. P., Nanoparticle polymer composites: Where two small worlds meet. *Science* 2006, *314* (5802), 1107-1110; (d) Qi, L.; Lee, B. I.; Chen, S. H.; Samuels, W. D.; Exarhos, G. J., High-dielectric-constant silver-epoxy composites as embedded dielectrics. *Adv Mater* 2005, *17* (14), 1777-+; (e) Vural, M.; Crowgey, B.; Kempel, L. C.; Kofinas, P., Nanostructured flexible magneto-dielectrics for radio frequency applications. *J Mater Chem C* 2014, *2* (4), 756-763; (f) Vural, M.; Behrens, A. M.; Ayyub, O. B.; Ayoub, J. J.; Kofinas, P., Sprayable Elastic Conductors Based on Block Copolymer Silver Nanoparticle Composites. *Acs Nano* 2015, *9* (1), 336-344.
2. (a) Yang, T. I.; Brown, R. N. C.; Kempel, L. C.; Kofinas, P., Magneto-dielectric properties of polymer-Fe(3)O(4) nanocomposites. *J Magn Magn Mater* 2008, *320* (21), 2714-2720; (b) Yang, T. I.; Brown, R. N. C.; CKempel, L.; Kofinas, P., Controlled synthesis of core-shell iron-silica nanoparticles and their magneto-dielectric properties in polymer composites. *Nanotechnology* 2011, *22* (10); (c) Morales, C.; Dewdney, J.; Pal, S.; Stojak, K.; Srikanth, H.; Wang, J.; Weller, T., Magnetically Tunable Nanocomposites for Microwave Applications. *Ieee Mtt S Int Micr* 2010; (d) Wu, L. Z.; Ding, J.; Jiang, H. B.; Chen, L. F.; Ong, C. K., Particle size influence to the microwave properties of iron based magnetic particulate composites. *J Magn Magn Mater* 2005, *285* (1-2), 233-239.
3. (a) Shen, Y.; Yue, Z. X.; Li, M.; Nan, C. W., Enhanced initial permeability and dielectric constant in a double-percolating Ni0.3Zn0.7Fe1.95O4-Ni-Polymer composite. *Adv Funct Mater* 2005, *15* (7), 1100-1103; (b) Guo, Z.; Lee, S. E.; Kim, H.; Park, S.; Hahn, H. T.; Karki, A. B.; Young, D. P., Fabrication, characterization and microwave properties of polyurethane nanocomposites reinforced with iron oxide and barium titanate nanoparticles. *Acta Mater* 2009, *57* (1), 267-277; (c) Dosoudil, R.; Usakova, M.; Franek, J.; Slama, J.; Olah, V., RF electromagnetic wave absorbing properties of ferrite polymer composite materials. *J Magn Magn Mater* 2006, *304* (2), E755-E757.
4. Lebourgeois, R.; LeFur, C.; Labeyrie, M.; Pate, M.; Ganne, J. P., Permeability mechanisms in high frequency polycrystalline ferrites. *J Magn Magn Mater* 1996, *160*, 329-332.
5. Song, N. N.; Yang, H. T.; Liu, H. L.; Ren, X.; Ding, H. F.; Zhang, X. Q.; Cheng, Z. H., Exceeding natural resonance frequency limit of monodisperse Fe3O4 nanoparticles via superparamagnetic relaxation. *Sci Rep-Uk* 2013, *3*.
6. Snoek, J. L., Dispersion and Absorption in Magnetic Ferrites at Frequencies above One Mc/S. *Physica* 1948, *14* (4), 207-217.
7. (a) Tartaj, P.; Morales, M. P.; Gonzalez-Carreno, T.; Veintemillas-Verdaguer, S.; Serna, C. J., The Iron Oxides Strike Back: From Biomedical Applications to Energy Storage Devices and Photoelectrochemical Water Splitting. *Adv Mater* 2011, *23* (44), 5243-5249; (b) Demortiere, A.; Panissod, P.; Pichon, B. P.; Pourroy, G.; Guillon, D.; Donnio, B.; Begin-Colin, S., Size-dependent properties of magnetic iron oxide nanocrystals. *Nanoscale* 2011, *3* (1), 225-232.
8. Yun, H.; Liu, X. Y.; Paik, T.; Palanisamy, D.; Kim, J.; Vogel, W. D.; Viescas, A. J.; Chen, J.; Papaefthymiou, G. C.; Kikkawa, J. M.; Allen, M. G.; Murray, C. B., Size- and Composition-Dependent Radio Frequency Magnetic Permeability of Iron Oxide Nanocrystals. *Acs Nano* 2014, *8* (12), 12323-12337.
9. (a) Baaziz, W.; Pichon, B. P.; Fleutot, S.; Liu, Y.; Lefevre, C.; Greneche, J. M.; Toumi, M.; Mhiri, T.; Begin-Colin, S., Magnetic Iron Oxide Nanoparticles: Reproducible Tuning of the Size and Nanosized-Dependent Composition, Defects, and Spin Canting. *J Phys Chem C* 2014, *118* (7), 3795-3810; (b) Batlle, X.; Perez, N.; Guardia, P.; Iglesias, O.; Labarta, A.; Bartolome, F.; Garcia, L. M.; Bartolome, J.; Roca, A. G.; Morales, M. P.; Serna, C. J., Magnetic nanoparticles with bulklike properties (invited). *J Appl Phys* 2011, *109* (7); (c) Daou, T. J.; Greneche, J. M.; Lee, S. J.; Lee, S.;

Lefevre, C.; Begin-Colin, S.; Pourroy, G., Spin Canting of Maghemite Studied by NMR and In-Field Mossbauer Spectrometry. *J Phys Chem C* 2010, *114* (19), 8794-8799.

10. (a) Lartigue, L.; Hugounenq, P.; Alloyeau, D.; Clarke, S. P.; Levy, M.; Bacri, J. C.; Bazzi, R.; Brougham, D. F.; Wilhelm, C.; Gazeau, F., Cooperative Organization in Iron Oxide Multi-Core Nanoparticles Potentiates Their Efficiency as Heating Mediators and MRI Contrast Agents. *Acs Nano* 2012, *6* (12), 10935-10949; (b) Yuan, H. L.; Wang, Y. Q.; Zhou, S. M.; Lou, S. Y., Fabrication of superparamagnetic Fe3O4 hollow microspheres with a high saturation magnetization. *Chem Eng J* 2011, *175*, 555-560; (c) Hu, P.; Yu, L. J.; Zuo, A. H.; Guo, C. Y.; Yuan, F. L., Fabrication of Monodisperse Magnetite Hollow Spheres. *J Phys Chem C* 2009, *113* (3), 900-906; (d) Xia, H. B.; Foo, P.; Yi, J. B., Water-Dispersible Spherically Hollow Clusters of Magnetic Nanoparticles. *Chem Mater* 2009, *21* (12), 2442-2451; (e) Wang, F. L.; Liu, J. R.; Kong, J.; Zhang, Z. J.; Wang, X. Z.; Itoh, M.; Machida, K., Template free synthesis and electromagnetic wave absorption properties of monodispersed hollow magnetite nano-spheres. *J Mater Chem* 2011, *21* (12), 4314-4320.

11. (a) Deng, H.; Li, X. L.; Peng, Q.; Wang, X.; Chen, J. P.; Li, Y. D., Monodisperse magnetic single-crystal ferrite microspheres. *Angew Chem Int Edit* 2005, *44* (18), 2782-2785; (b) Zhu, Y. F.; Zhao, W. R.; Chen, H. R.; Shi, J. L., A simple one-pot self-assembly route to nanoporous and monodispersed Fe3O4 particles with oriented attachment structure and magnetic property. *J Phys Chem C* 2007, *111* (14), 5281-5285.

12. Cheng, C. M.; Xu, F. J.; Gu, H. C., Facile synthesis and morphology evolution of magnetic iron oxide nanoparticles in different polyol processes. *New J Chem* 2011, *35* (5), 1072-1079.

13. Xuan, S. H.; Wang, Y. X. J.; Yu, J. C.; Leung, K. C. F., Tuning the Grain Size and Particle Size of Superparamagnetic Fe3O4 Microparticles. *Chem Mater* 2009, *21* (21), 5079-5087.

14. (a) Cheng, C. M.; Wen, Y. H.; Xu, X. F.; Gu, H. C., Tunable synthesis of carboxyl-functionalized magnetite nanocrystal clusters with uniform size. *J Mater Chem* 2009, *19* (46), 8782-8788; (b) Lin, M. H.; Huang, H. L.; Liu, Z. T.; Liu, Y. J.; Ge, J. B.; Fang, Y. P., Growth-Dissolution-Regrowth Transitions of Fe3O4 Nanoparticles as Building Blocks for 3D Magnetic Nanoparticle Clusters under Hydrothermal Conditions. *Langmuir* 2013, *29* (49), 15433-15441.

15. Liu, H. F.; Ji, S. F.; Zheng, Y. Y.; Li, M.; Yang, H., Modified solvothermal synthesis of magnetic microspheres with multifunctional surfactant cetyltrimethyl ammonium bromide and directly coated mesoporous shell. *Powder Technol* 2013, *246*, 520-529.

16. Goyal, A.; Kumar, A.; Patra, P. K.; Mahendra, S.; Tabatabaei, S.; Alvarez, P. J. J.; John, G.; Ajayan, P. M., In situ Synthesis of Metal Nanoparticle Embedded Free Standing Multifunctional PDMS Films. *Macromol Rapid Comm* 2009, *30* (13), 1116-1122.

17. (a) Schadler, L. S.; Kumar, S. K.; Benicewicz, B. C.; Lewis, S. L.; Harton, S. E., Designed interfaces in polymer nanocomposites: A fundamental viewpoint. *Mrs Bull* 2007, *32* (4), 335-340; (b) Fu, S. Y.; Feng, X. Q.; Lauke, B.; Mai, Y. W., Effects of particle size, particle/matrix interface adhesion and particle loading on mechanical properties of particulate-polymer composites. *Compos Part B-Eng* 2008, *39* (6), 933-961; (c) Bartczak, Z.; Argon, A. S.; Cohen, R. E.; Weinberg, M., Toughness mechanism in semi-crystalline polymer blends: II. High-density polyethylene toughened with calcium carbonate filler particles. *Polymer* 1999, *40* (9), 2347-2365.

18. Choi, K. M.; Rogers, J. A., A photocurable poly(dimethylsiloxane) chemistry designed for soft lithographic molding and printing in the nanometer regime. *J Am Chem Soc* 2003, *125* (14), 4060-4061.

19. Brosseau, C.; Ben Youssef, J.; Talbot, P.; Konn, A. M., Electromagnetic and magnetic properties of multicomponent metal oxides heterostructures: Nanometer versus micrometer-sized particles. *J Appl Phys* 2003, *93* (11), 9243-9256.

20. Kittel, C., On the Theory of Ferromagnetic Resonance Absorption. *Phys Rev* 1948, *73* (2), 155-161.

21. Konn, A. M.; Laurent, P.; Talbot, P.; Lefloch, M., Study of Relaxation and Spin-Resonance in Magnetic Liquids. *J Magn Magn Mater* 1995, *140*, 367-368.

22. Aragon, R., Cubic Magnetic-Anisotropy of Nonstoichiometric Magnetite. *Phys Rev B* 1992, *46* (9), 5334-5338.